

# Hydraulic Fracturing of the Floridan Aquifer from Aquifer Storage and Recovery Operations

NICHOLAS M. GEIBEL

*U.S. Army Corps of Engineers, Omaha District, 1616 Capitol Avenue, Omaha, NE  
68102*

CHRISTOPHER J. BROWN

*Department of Civil Engineering, 1 UNF Drive, University of North Florida,  
Jacksonville, FL 32224*



**Key Terms:** *Aquifer Storage and Recovery, Hydraulic Fracturing, Rock Mechanics, Floridan Aquifer System, Triaxial Compressive Strength, Unconfined Compressive Strength*

## ABSTRACT

Potential for hydraulically induced fracturing of the Floridan Aquifer System (FAS) and the overlying Hawthorn Group deposit exists due to operation of seven potential aquifer storage and recovery facilities planned to be developed in south-central Florida to enhance Everglades restoration. The purpose of this study was to determine critical threshold water pressures at which hydraulically induced fracturing of the FAS rock matrix may occur. Several FAS rock matrix samples were collected, tested, and evaluated to define representative mechanical properties, which were then used in relation with *in situ* stresses to determine critical threshold water pressures. Three hydraulically induced fracturing failure mode evaluation methods based on shear, tensile, and microfracture development were utilized. Microfracture development requires the lowest critical threshold water pressure to induce fracturing, followed by tensile and then shear failure modes. Predictive critical threshold water pressures for tensile and microfracture development failure modes can potentially be achieved during full-scale operation of the planned aquifer storage and recovery facilities; therefore, appropriate design considerations and operational precautions should be taken to minimize water pressures that exceed this operational constraint. If hydraulically induced fractures are developed in the FAS, their propagation into the Hawthorn Group deposit would likely be arrested by or re-directed along the discontinuity zone at the contact of these two deposits. Additionally, the Hawthorn Group deposit exhibits a significantly lower modulus of elasticity than the FAS, which would tend to effectively arrest hydraulically induced fracture propagation.

## INTRODUCTION

A portion of the April 1999 Comprehensive Everglades Restoration Plan (CERP) includes a proposed large-scale development of aquifer storage and recovery (ASR) facilities throughout southern Florida to provide additional freshwater storage for Lake Okeechobee, its tributaries, and the Greater Everglades Ecosystem (U.S. Army Corps of Engineers [USACE] and South Florida Water Management District [SFWMD], 1999). As currently proposed, the CERP ASR system includes up to 333 ASR wells and associated surface facilities at multiple sites. During periods when the quantity of surface water is sufficient to meet the environmental needs of the Everglades ecosystem, the wells will be used to inject, or recharge, treated surface water into the Floridan Aquifer System (FAS) for storage, and conversely during low-water conditions, the same wells will be used to recover water from the FAS to replenish surface waters of the ecosystem. Each proposed ASR well has a target recharge capacity of 5 million gallons ( $1.9 \times 10^7$  L) of treated water per day and a variable recovery rate depending on surface-water needs.

The USACE and SFWMD are evaluating the feasibility of the proposed CERP ASR system through the construction and testing of pilot ASR wells and surface-water treatment systems, along with the development of a comprehensive regional feasibility study. One component of the feasibility study is to determine the hydraulically induced fracturing potential of the FAS and overlying Hawthorn Group deposit from an anticipated daily ASR recharge or recovery volume of 1.67 billion gallons ( $6.3 \times 10^9$  L) of water.

The magnitude of the increase/decrease in hydraulic pressure within the upper portions of the FAS during recharge/recovery ASR operational cycles, respectively, is highly dependent upon a number of factors, such as transmissivity of the FAS, well

spacing, and injection and recovery rates. During ASR operational recharge phases, increases of 100 to 200 feet (ft) (31 to 61 m) in static hydraulic head in the FAS within the areas of the ASR well fields are possible (Brown et al., 2005; Brown, 2007). Conversely, during ASR recovery phases, similar decreases in magnitude of the static hydraulic head are possible. These hydraulic pressure changes will need to be considered during the evaluation of planning and engineering constraints that may limit ASR system design and operation. An effect of large-scale ASR operation is the potential for hydraulically induced fracturing of the limestone rock matrix of the FAS and the overlying Hawthorn Group deposit. Hydraulically induced fracturing of the FAS may locally increase its transmissivity and actually enhance practical ASR operational recharge and recovery rates.

Hydraulic fracturing was developed during the 1930s and 1940s by the oil industry as a means to enhance production of oil wells. During these early years of development and deployment, hydraulically induced fracturing was thought to occur when the hydraulic pressure at any specific point in the well reached or just exceeded the pressure due to the weight of the overburden at that point (which is considered to be about 1 pound per square inch [psi] per foot [0.023 MPa/m] of overburden) (Bouwer, 1978; Smith, 1989). Since these early developments, it has been shown through numerous research and field application efforts that hydraulically induced fracturing can be initiated at pressures ranging from much lower to somewhat higher than the local overburden pressure and that it is related to rock strength parameters and alignment and magnitude of *in situ* stresses. As reported by Driscoll (1986), hydraulic pressures that caused fracturing ranged from a low of 0.5 psi/ft (0.011 MPa/m) of depth in poorly consolidated coastal plain sediments to 1.2 psi/ft (0.027 MPa/m) of depth for crystalline rock. Bouwer (1978) indicated that hydraulically induced fracturing could be initiated at a pressure as low as 50 percent of the overburden pressure, but more typically the pressure should not exceed 67 percent of the overburden pressure in order to reduce fracturing potential. Recent oil industry guidelines discussed by Ehlig-Economides and Economides (2010) indicated that almost all reservoirs will hydraulically fracture within a range from 0.71 to 0.82 psi/ft (0.015 MPa/m to 0.018 MPa/m) of depth. As a rough guide, drilling professionals trying to induce hydraulic fracturing estimate required down-hole injection pressures of 1 psi/ft (0.023 MPa/m) of depth plus an additional 1,500 psi (10.3 MPa) (Sterrett, 2007). Overall, these general hydraulically induced fracturing criteria

envelope a wide range of injection pressures that could initiate the onset of fracturing for wide ranges of *in situ* states of stress and rock matrix types. Therefore, we need to calculate site-specific hydraulic pressures, or water pressures, that may initiate the onset of hydraulically induced fracturing based on FAS rock matrix mechanical properties and *in situ* stress conditions in order to develop ASR facility design and operational criteria.

The purpose of this study was to determine critical threshold water pressures at which the onset of hydraulically induced fracturing of the FAS rock matrix may occur and their implications for fracturing the Hawthorn Group deposit at each potential ASR site. The evaluation of potential hydraulically induced fracturing of the FAS and Hawthorn Group deposit was accomplished for seven potential ASR sites: Caloosahatchee River, Moorehaven, Kissimmee River, Port Mayaca, Hillsboro, Seminole-Brighton, and Paradise Run (Figure 1).

## HYDROGEOLOGIC SETTING

There are three principal hydrogeologic systems in south Florida; in descending stratigraphic order, they are: the Surficial Aquifer System (SAS), the Hawthorn Group deposit, and the FAS. Within each of these hydrogeological systems, there are confining units. Additionally, depending on the lithologic makeup of the Hawthorn Group deposit, it may act as an aquifer, termed the Intermediate Aquifer System (IAS), or as a much less permeable deposit acting predominantly as a confining unit effectively separating the SAS and the FAS.

Across the study area, the SAS typically consists of series of deposits that are hydraulically connected unconfined and semi-confined aquifers of Pleistocene and Pliocene age. These deposits are composed of loose, sandy materials; sandy and shelly porous limestone; and sandstone and silts that exhibit a wide range of permeabilities, and that are divided into distinct aquifers separated by less permeable units that serve as semi-confining layers. The individual aquifers that make up the SAS tend to be discontinuous and locally productive, reflecting the overall complex stratigraphic nature of this aquifer system. The thickness of the SAS varies from approximately 32 to 210 ft (10 to 64 m) at the potential ASR sites.

As previously stated, the Hawthorn Group deposit exhibits characteristics of either an aquifer consisting of beds of sand, sandy limestone, limestone and dolostone, silt, and clay, or a confining unit (Fernald and Purdum, 1998). The IAS portion of the Hawthorn Group deposit pinches out in the southern and eastern portions of Florida, including the study

## Fracturing the Floridan Aquifer

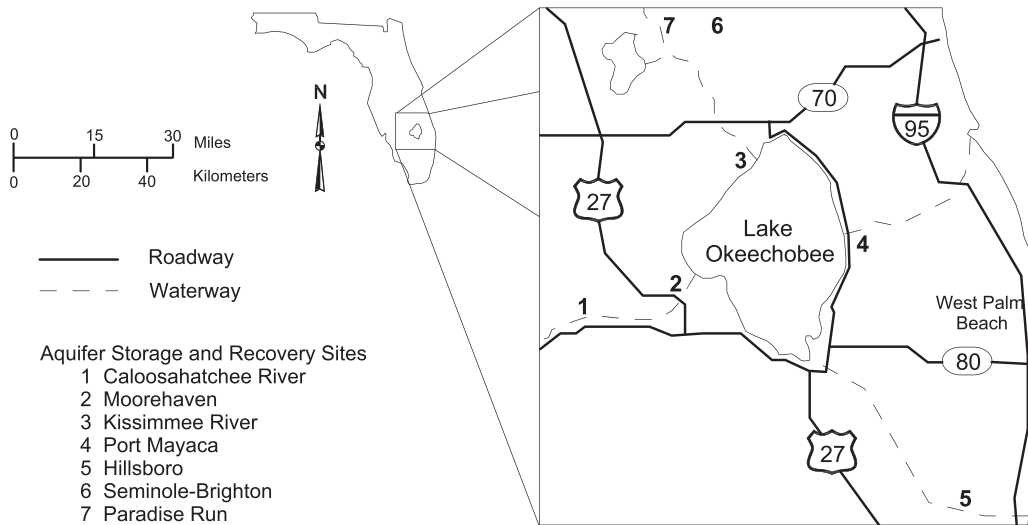


Figure 1. Locations of potential aquifer storage and recovery sites in Florida identified for the Comprehensive Everglades Restoration Plan.

area, where the clay content of the deposit increases and it acts as a confining unit separating the SAS and FAS. In the study area, the stratigraphic makeup of the Hawthorn Group deposit is complex, exhibiting numerous inter-fingering thin units of fine-grained, low-permeability sediments and some limestone layers (Scott, 2001). Clay units within the Hawthorn Group deposit have been characterized as variable and include both kaolinite and smectite mineral types, which exhibit a deformable nature. The thickness of the Hawthorn Group deposit varies from approximately 396 to 735 ft (121 to 224 m) at the potential ASR sites.

The FAS is a thick sequence of Paleocene- to Miocene-age carbonate units underlying the entire state of Florida. The upper part of the Cedar Keys Formation, Oldsmar Formation, Avon Park Formation, Ocala Limestone, Suwannee Limestone, and the lower portion of the Arcadia Formation are included in the FAS (Miller, 1986; Reese, 2000). Low-permeability anhydrite units in the lower portion of the Cedar Keys Formation constitute the base of the FAS. The FAS, a source for primary water supply and supplemental irrigation water, dips to the south, where it is overlain by clays and silts of the Hawthorn Group deposit. A confining unit is present in the middle of the FAS, effectively dividing it into upper and lower units. The middle confining unit consists of a less permeable carbonate unit relative to the upper and lower units.

In the vicinity of the study area, the potentiometric surface of the FAS rises above land surface to 40 to 55 ft (12 to 17 m) mean sea level (msl), resulting in artesian conditions as wells freely flow up to 2,000 gallons per minute (126 L/s). North of Lake Okeecho-

bee, the FAS yields freshwater, which becomes more mineralized (total dissolved solids >1,000 mg/L) along coastal areas and throughout southern Florida. Although the hydraulic gradient in the FAS contains an upward component, the confining nature of the Hawthorn Group deposit prevents significant upward movement of brackish water from entering the SAS (Fernald and Purdum, 1998).

## METHODOLOGY

Three primary evaluation methods, termed shear, tensile, and microfracture, were used to determine critical threshold water pressures at which the potential onset of hydraulically induced fracturing will occur at a specific point in the FAS. Two additional evaluation methods to determine hydraulically induced fracturing potential were also utilized to check the outcomes of the three primary methods. A typical ASR well will only inject or recover water directly into or out of the FAS, thereby imparting hydraulically induced fracture driving stresses to the FAS. Stress due to the weight of overburden is the primary stress resisting hydraulically induced fracturing, which, within the FAS, exhibits its lowest magnitude at the top of the FAS, rendering this point the most vulnerable to the onset of hydraulically induced fracturing and making it the evaluation point of interest. For the three primary methods, a factor of safety (FS) of 10 percent was applied to the predictive hydraulically induced fracturing results to account for assumptions applied to the evaluations and to define ASR design and operational water-pressure thresholds above which caution should be exercised.

Several other factors may influence FAS rock matrix stability, rendering it more or less susceptible to hydraulically induced fracturing due to installation of a well borehole or ASR operational recharge and recovery phases; these include: (1) resultant stress intensity on the well borehole wall due to decreasing water pressure in the well (Aadnoy, 1996), (2) magnitude redistribution of the pre-drilling *in situ* principal stress field around the well borehole (Fjar et al., 2008), (3) chemical dissolution or precipitation of FAS rock matrix, and (4) fatigue failure of the well borehole wall due to cyclic ASR operations (Haimson, 1978; Higdon et al., 1985; Singh, 1989; Alehossein and Boland, 2004; and Zhang et al., 2008). The effects, whether positive or negative, of these four factors on the initiation of hydraulically induced fracturing will likely be very minimal and confined to the rock matrix at and very near the well borehole wall and are considered minor limitations of the methodology.

Hydraulically induced fracturing of the Hawthorn Group deposit, if realized, would be the result of vertical upward propagation of fractures initiated within the FAS. Direct hydraulically induced fracturing of the Hawthorn Group deposit due to ASR operation is not possible because water will not be recharged or recovered directly into or out of the Hawthorn Group deposit, thereby eliminating the source of stress that could initiate fracturing of the deposit. To determine potential hydraulically induced fracturing of the Hawthorn Group deposit, a propagation arrest model was applied to the potential ASR sites. The model considers geologic, formation elasticity, and *in situ* stress factors that influence arrest of propagating hydraulic fractures.

#### *In Situ* State of Stresses

To understand the potential for and orientation of hydraulically induced fracturing, the *in situ* state of the regional stress field must be evaluated. In a regional stress field, there exists within a geologic unit a stress point intersected by three orthogonal planes, called principal planes. A stress component is aligned normal to each of these planes: They are termed the maximum ( $\sigma_1$ ), intermediate ( $\sigma_2$ ), and minimum ( $\sigma_3$ ) principal stresses. Under near-horizontal ground that is not subjected to significant tectonic forces,  $\sigma_1$  will be oriented in the vertical direction, while  $\sigma_2$  and  $\sigma_3$  will be oriented in the horizontal direction. These stresses will be compressive in nature simply due to the weight of the overlying geologic materials, confinement, and fluid pressure if fluid is present. Under *in situ* conditions where the regional stress field is subjected to significant tectonic forces, such as

faulting, or influences from significantly uneven topographic ground conditions,  $\sigma_1$  and associated  $\sigma_2$  and  $\sigma_3$  may not be oriented in the vertical and horizontal directions, respectively (Goodman, 1980). A review of the world stress map for the study area indicated that tectonically induced stress does not appear to be prevalent as exhibited by the lack of stress indicators in the study region (Heidbach et al., 2008). However, this lack of tectonic stress indicators may be due to an incomplete stress-indicator data set for the region. All ASR project sites have nearly horizontal ground conditions with no major topographic change and are not subjected to significant tectonic activity; therefore, it is assumed that the *in situ* states for  $\sigma_1$  and associated  $\sigma_2$  and  $\sigma_3$  are oriented in the near-vertical and horizontal directions, respectively.

In many cases,  $\sigma_2$  is near or equal in magnitude to  $\sigma_3$ , allowing for a two-dimensional stress analysis (Rahn, 1986), which is an acceptable evaluation criterion for the proposed ASR sites based on the directional distribution of the *in situ* regional stress field. If  $\sigma_2$  is significantly greater in magnitude than  $\sigma_3$ , the use of three-dimensional analysis may be warranted because a two-dimensional analysis may over- or under-predict the effects of applied forces. General conceptual hydrogeologic conditions assumed for the ASR project sites along with a two-dimensional stress element showing the orientations of the principal stresses at the top of the FAS are shown on Figure 2A. In addition to the principal stresses acting on the element, shear and normal stresses are acting on planes oriented at all angles within the stress element as a result of the influence of the principal stresses. Along an internal plane oriented at some angle in the stress element, a shear stress,  $\tau_\theta$ , provides a force acting tangential to the plane, while a normal stress,  $\sigma_\theta$ , provides a force acting normal to the plane, as shown on Figure 2B. Shear stresses are not associated with planes upon which principal stresses act.

#### Shear Method

The shear method involves an analysis of shear stresses developed as a result of the principal stresses acting at the evaluation point of interest. Ultimately, the shear strength of the FAS rock matrix and the shear stress acting on a critical failure plane are determined and compared. If the imposed shear stress is greater than the shear strength of the FAS rock matrix, the potential for hydraulically induced fracturing along some critical failure plane within the FAS rock matrix exists. Fracturing due to shear may be induced at the well borehole wall or at any

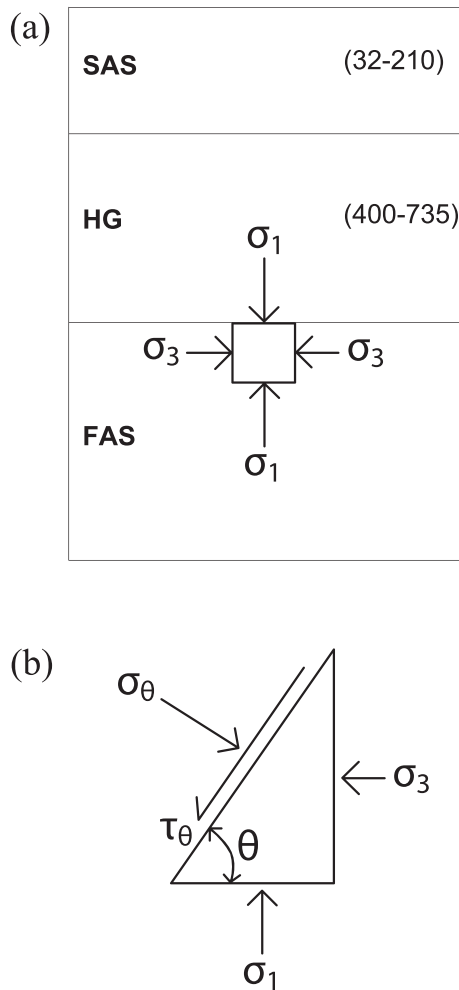


Figure 2. (a) Hydrogeological conceptual site conditions for the potential aquifer storage and recovery sites. The range of thickness in feet is shown in parentheses for the Surficial Aquifer System (SAS) and Hawthorn Group sediments (HG). The stress element at the evaluation point of interest at the top of the Floridan Aquifer System (FAS) indicates the orientation of the maximum ( $\sigma_1$ ) and minimum ( $\sigma_3$ ) principal stresses. (b) Shear ( $\tau_\theta$ ) and normal ( $\sigma_\theta$ ) stresses acting along an internal plane oriented at some angle ( $\theta$ ) within the stress element. 1 ft = 0.3048 m.

point within the FAS when hydraulic pressure conditions favor failure.

The shear strength,  $S_\tau$  (Force/Length<sup>2</sup> [F/L<sup>2</sup>]), of the FAS rock matrix along some critical failure plane at an evaluation point of interest was determined utilizing the following Mohr-Coulomb equation (Terzaghi and Peck, 1967; Jaeger et al., 2007):

$$S_\tau = C + (\sigma_\theta - P) \tan \Phi \quad (1)$$

where  $C$  is cohesive strength of FAS rock matrix [F/L<sup>2</sup>],  $\sigma_\theta$  is stress normal to the potential failure plane [F/L<sup>2</sup>],  $P$  is water pressure [F/L<sup>2</sup>], and  $\Phi$  is angle of internal friction of FAS rock matrix (in degrees). The

Mohr-Coulomb criterion is a linear function of the rock-failure, or stress, envelope (Goodman, 1980). To determine  $P$  at the evaluation point of interest, the following relationships are used:

$$P = \gamma_w \times PH \quad (2)$$

where  $\gamma_w$  is specific weight of water [F/L<sup>3</sup>], and  $PH$  is pressure head [L]. The value of  $PH$  for the evaluation point of interest can be determined using the following form of Bernoulli's equation in terms of hydraulic head:

$$TH = EH + PH + VH \quad (3)$$

where  $TH$  is total head [L],  $EH$  is elevation head [L], and  $VH$  is velocity head [L]. The  $VH$  term is very small relative to the  $TH$ ,  $EH$ , and  $PH$  terms due to the extremely slow rate of groundwater movement and can therefore be considered negligible and removed from the equation. Measurements of  $TH$ ,  $EH$ , and  $PH$  are made from some consistent datum, which will be msl for purposes of this evaluation. Solving Eq. 3 for  $PH$  yields:

$$PH = TH - EH \quad (4)$$

The following Mohr circle formulation can be used to determine the magnitude of  $\sigma_\theta$ , a component in Eq. 1, acting on the critical failure plane (Rahn, 1986; American Society for Testing and Materials [ASTM], 2007 [D 7012]):

$$\sigma_\theta = [(\sigma_v + \sigma_H)/2] + [(\sigma_v - \sigma_H)/2] \cos 2\theta \quad (5)$$

where  $\sigma_v$  is total overburden stress [F/L<sup>2</sup>],  $\sigma_H$  is total horizontal stress [F/L<sup>2</sup>], and  $\theta$  is angle of the critical failure plane ( $45^\circ + \Phi/2$ ) [in degrees]. Simply based on nomenclature, the principal stresses  $\sigma_1$  and  $\sigma_3$  are synonymous to  $\sigma_v$  and  $\sigma_H$ , respectively, due to vertical and horizontal orientation. The critical failure plane upon which hydraulically induced fracturing, illustrated in Figure 2B, is likely to occur develops at an angle,  $\theta$ , of  $45^\circ + \Phi/2$  from  $\sigma_H$  (Hubbert and Willis, 1957; Blyth and de Freitas, 1984).

The total overburden stress,  $\sigma_v$ , is due to the weight of the overburden at the evaluation point of interest and is defined by:

$$\sigma_v = \sum_{i=1}^n \gamma_i \times h_i \quad (6)$$

where  $\gamma_i$  is the specific weight of the geologic unit at its natural moisture content [F/L<sup>3</sup>], and  $h_i$  is the

thickness of the geologic unit [L]. The following relationship is used to determine  $\sigma_H$  according to Terzaghi's effective stress law (Rutqvist and Stephansson, 2003):

$$\sigma_H = \sigma_{\text{Heff}} + P \quad (7)$$

where  $\sigma_{\text{Heff}}$  is horizontal effective stress [ $F/L^2$ ]. The stress field component,  $\sigma_{\text{Heff}}$ , results from the  $\sigma_H$  force acting upon the FAS rock matrix, while  $P$  (described in Eq. 1 and Eq. 2) is the stress field component of  $\sigma_H$  resulting from the forces acting upon water in the pore spaces of the FAS rock matrix. Utilizing the following relation,  $\sigma_{\text{Heff}}$  can be estimated:

$$\sigma_{\text{Heff}} = K_o \times \sigma_{\text{Veff}} \quad (8)$$

where  $\sigma_{\text{Veff}}$  is vertical effective stress [ $F/L^2$ ], and  $K_o$  is the coefficient of lateral earth pressure. At the potential ASR sites, a reasonable estimate of  $K_o$  can be determined by:

$$K_o = 1 - \sin \Phi \quad (9)$$

The stress field component  $\sigma_{\text{Veff}}$  results from the  $\sigma_V$  force acting upon the FAS rock matrix, while  $P$  (described in Eq. 1 and Eq. 2) is the stress field component of  $\sigma_V$  resulting from the forces acting upon water in the pore spaces of the FAS rock matrix and can be determined by:

$$\sigma_{\text{Veff}} = \sigma_V - P \quad (10)$$

To determine the shear stress,  $\tau_\theta$  [ $F/L^2$ ], acting along a critical failure plane at an angle  $\theta$  at a point of interest in the FAS, the following Mohr circle formulation is utilized (Rahn, 1986; ASTM, 2007 [D 7012]):

$$\tau_\theta = [(\sigma_V - \sigma_H)/2] \sin 2\theta \quad (11)$$

This method can be used to evaluate an incremental series of shear strengths and shear stresses at corresponding  $P$  values for the FAS evaluation point of interest. By plotting respective shear strengths and shear stresses at corresponding  $P$  values, the  $P$  at which hydraulically induced fracture onset will occur can be determined by identifying the critical threshold shear stress that exceeds the shear strength of the rock.

#### Tensile Method

Hydraulic fracturing at a particular point on a well borehole wall will be induced when the pressure of the

fluid in the well exceeds  $\sigma_3$  by an amount equal to the tensile strength of the rock. After a hydraulic fracture is induced into the borehole wall, a small, localized, heterogeneous stress field is formed at its tip and controls its propagation. The fracture geometry and loading configuration, termed the stress intensity factor, control the magnitude of the stress field. Microfractures will develop within the stress field when its magnitude is sufficient, and the density of the microfractures increases as the magnitude of the stress field increases. The fracture toughness of the rock matrix is a resisting force against fracture propagation. Fracture toughness is related to rock matrix properties such as strength, composition, and temperature, and during laboratory rock specimen testing, the applied rate of loading and magnitude of the confining pressure. At a critical stress intensity level, where the stress intensity factor is equal to or greater than the fracture toughness, the hydraulic fracture will propagate as the individual microfractures coalesce to form a macrofracture within the fracture tip stress field (Pollard and Aydin, 1988).

Theoretically, the induced hydraulic fracture plane will be generated and propagate parallel to the principal stress axes of  $\sigma_1$  and  $\sigma_2$  and will therefore be perpendicular to the  $\sigma_3$  stress axis (Goodman, 1980; Rahn, 1986; Smith, 1989; Domenico and Schwartz, 1998; and Jaeger et al., 2007). Fracture plane orientation and propagation align generally with the principal stress axes as described previously and thus will align as such relative to the orientation of any principal stress axes (e.g., if  $\sigma_3$  is aligned vertically, then the fracture plane orientation and propagation will be horizontal). In addition to the vertical propagation alignment of the induced hydraulic fracture (assuming  $\sigma_1$  and  $\sigma_3$  axes are in vertical and horizontal alignment, respectively), the fracture will propagate radially from the well. According to Smith (1989), the orientation and propagation of fractures can also be influenced by anisotropy or planar inhomogeneities in the rock (i.e., bedding, schistosity, cleavage, joints, etc.). Fracture orientation and propagation may potentially parallel these types of features. The stress field at the tip of a fracture may influence an adjacent fracture's stress field tip and thus its propagation path and orientation (Pollard et al., 1982). Jaeger et al. (2007) suggests that the fractures may be irregular and discontinuous in nature; that is, they may not initiate or propagate along the entire length of a fracture plane.

The tensile method, developed by Hubbert and Willis (1957), involves an analysis of a critical stress level relative to some  $P$ , acting at the evaluation point of interest, that is required to initiate hydraulically induced fracturing of a well borehole wall as

described already. If, at some evaluation point of interest, the  $P$  within the well borehole is equal to or greater than the critical water-pressure stress level for the well borehole wall, the potential for hydraulic fracturing of the well borehole wall and FAS rock matrix exists. The critical water-pressure stress level,  $P^f$  [ $F/L^2$ ], at an evaluation point of interest, of the FAS rock matrix at the well borehole wall is determined utilizing the following equation (Hubbert and Willis, 1957):

$$P^f = (\sigma_v \times M) - P_a \times (M - 1) \quad (12)$$

where  $P_a$  is ambient pre-fracture water pressure [ $F/L^2$ ]. Equation 6 is used to determine  $\sigma_v$ , and  $M$  is the ratio of horizontal to vertical stress, which is equivalent to  $K_0$  and is determined using Eq. 9. Actual values of  $P$  within the well borehole at the evaluation point of interest are determined using Eq. 2 for various incremental head changes. By plotting a series of values representing incremental  $P$  values within the well borehole at the evaluation point of interest and comparing them to  $P^f$ , the  $P$  at which hydraulic-fracture onset will occur can be determined when  $P$  equals  $P^f$ .

#### Microfracture Method

The microfracture method provides a way to evaluate the hydraulically induced microfracturing potential of FAS rock matrix due to water-pressure conditions. Handin et al. (1963) suggested that abnormally high  $P$  results in dilatancy effects within the rock matrix. Dilatancy is the change in volume of a material when subject to shearing or other deformation forces. As the rock matrix dilates due to increasing  $P$ , the pore volume increases and may materialize in the form of microfractures (Palciauskas and Domenico, 1980). The resultant force causing the dilatancy effect on the pore space of the rock matrix is oriented parallel to the  $\sigma_1$  and  $\sigma_2$  principal stress axes and perpendicular to the  $\sigma_3$  stress axis; therefore, resulting microfractures are oriented and propagate in a similar way to hydraulic fracture orientation and propagation described under the tensile method. Upon the development of microfractures, the excess  $P$  that initiated the dilatancy effect tends to be relieved (Keith and Rimstidt, 1985). However, if  $P$  continues to increase and cannot be sufficiently relieved by the existing microfracture network or other means, the microfractures will expand, and/or additional microfractures will develop. As individual microfractures propagate or their density increases, they can combine and lead to well-developed macrofracture planes (Sherman, 1973; Jaeger et al., 2007).

After the macrofracture planes are developed, failure will likely occur and may be initiated at the well borehole wall or at any point within the FAS that exhibits appropriate dilatancy conditions.

To evaluate the microfracture failure criterion at the evaluation point of interest, the following empirical relations are used (Handin et al., 1963):

$$\text{HDR} = P/\sigma_H \quad (13)$$

where HDR is Handin Dilatancy Ratio (HDR), and  $P$  and  $\sigma_H$  are determined using Eq. 2 and Eq. 7, respectively. The HDR at which dilatancy is initiated, resulting in the onset of microfracturing, differs for various rock types. For sedimentary rocks, such as those of the FAS, dilatancy is observed when HDR is approximately 0.8 (Handin et al., 1963). Therefore, for the purposes of this microfracturing failure criterion, 0.8 will be considered the critical level for HDR at which the onset of dilatancy and microfracture development will occur and be termed the Limiting Handin Dilatancy Ratio (LHDR). It should be noted that this microfracture failure criterion is supported by actual FAS laboratory rock testing stress-strain results. By plotting a series of HDR values at associated  $P$  values and comparing them to the LHDR, the  $P$  at which microfracture onset will occur can be determined.

#### Check Methods

Goodman (1980) presented a method based on the Mohr-Coulomb linear failure criterion in terms of principal stresses at peak load condition to determine the  $P$  in pores and fissures required to initiate fracture of intact rock. Calculation of  $P$  is based on an initial state of stresses, defined by  $\sigma_v$  and  $\sigma_H$  at some evaluation point of interest. The hydraulic fracture-inducing  $P$  can be determined using the following equation:

$$P = \sigma_H - \{[(\sigma_v - \sigma_H) - qu]/[\tan^2(45^\circ + \Phi/2) - 1]\} \quad (14)$$

where  $qu$  is unconfined compressive strength [ $F/L^2$ ] of the intact rock matrix. The mechanical property  $qu$  is determined through testing FAS rock matrix samples in an unconfined manner. Resultant fracture-inducing  $P$  values calculated by this check method can be compared to ensure that predictive  $P$  values calculated by the shear method are not grossly over- or under-represented.

A second check method considers initiation of hydraulically induced fracturing, either at a well borehole wall or within the FAS, when the fluid pressure at the evaluation point of interest is equal to

50 to 67 percent of  $\sigma_v$  (Bouwer, 1978). To determine the critical fluid pressure required to initiate hydraulic fracturing, Eq. 6 is used to calculate  $\sigma_v$  at 100 percent, which is then multiplied by the desired fluid pressure percentage factor, resulting in  $\sigma_{v\%}$  [F/L<sup>2</sup>]. The following relation is used to determine the height of fluid column,  $h_f$  [L], required to equal  $\sigma_{v\%}$ :

$$h_f = \sigma_{v\%} / \gamma_f \quad (15)$$

where  $\gamma_f$  is the specific weight of the fluid [F/L<sup>3</sup>]. The resultant  $h_f$  values calculated using this check method can be converted to like terms and compared with the hydraulically induced fracturing predictive  $P^f$  and TH values determined using the tensile and microfracture methods, respectively, assuring results are not grossly over- or under-represented.

### Hydraulically Induced Fracture Propagation Arrest Model

A criterion of ASR design and operation is to minimize the potential to hydraulically induce fracturing of the Hawthorn Group deposit. Hydraulically induced fracturing of the Hawthorn Group deposit may allow uncontrolled recharge distribution and be detrimental to the recovery phase efficiency of ASR operations. Hydraulically induced fracturing of the Hawthorn Group deposit, if realized, would be the result of vertical propagation of fractures initiated within the FAS. Gudmundsson and Brenner (2001) present a model of hydraulically induced fracture propagation arrest. According to their model, arrest of hydraulically induced fracture propagation is a function of three factors: discontinuities, variations in the modulus of elasticity ( $E$ ) within or between geological layers, and stress barriers. Any single or combination of these three factors has the ability to redistribute the fracture-promoting hydraulically induced stress field at the tip of a propagating fracture. It is the redistribution of the stress field intensity that allows the hydraulically induced fracture to potentially be redirected and ultimately become arrested.

A discontinuity is a feature that exhibits low or negligible tensile strength, such as a defined contact between two differing geological materials. A pre-existing discontinuity will prevent the stress perturbation associated with the propagating crack tip from being transmitted across the discontinuity. Therefore, the hydraulic fracture will become arrested or propagate some distance along the plane of the discontinuity rather than continue across the discontinuity.

A laboratory testing or field-derived value,  $E$  describes the amount of axially applied stress that is

required to achieve a given amount of axial elastic shortening of a core of rock, acting as a measure of the stiffness of the rock. The greater the stiffness of the deposit, the greater is the value of  $E$ . Hydraulic fracture propagation has a tendency to be arrested at the contact of two geological materials exhibiting substantially different values of  $E$  (Gudmundsson and Brenner, 2001). When a hydraulic fracture encounters a deposit exhibiting a substantially lower  $E$  than the fracture host deposit, the hydraulic fracture tip stress tends to dissipate in the lower  $E$  deposit to levels not conducive for continued fracture propagation and thus becomes arrested.

A stress barrier is a zone in which the compressive or tension stresses, aligned perpendicular to the direction of hydraulic fracture propagation, are greater or less than those observed in adjacent zones (Gudmundsson and Brenner, 2001). In the case of a compressive stress barrier, the hydraulic fracture tip stress is dissipated in such a manner that it penetrates only a short distance within the rock mass hosting the compressive stress barrier. Hydraulic fracture tip stress is dissipated in much the same manner in a tension stress barrier as it is in a compressive stress barrier. This redistribution of hydraulic fracture tip stress allows for a very limited distance of fracture propagation into the rock mass hosting the compressive or tension stress barrier, followed by arrest. An exception may be a tension stress barrier arresting fracture propagation due to shear.

### LABORATORY TESTING AND RESULTS

Mechanical and elastic properties of the rock matrix that are used in the hydraulically induced fracturing evaluation methods include  $\Phi$ ,  $C$ , and  $E$ . The methodology used to determine  $\Phi$  and  $C$  was through the development and evaluation of Mohr stress envelopes from various sets of laboratory rock strength testing results. In order to develop the Mohr stress envelopes,  $qu$  and triaxial compressive strength (TCS) laboratory testing results of FAS rock matrix specimens were utilized, and if available, tensile strength laboratory results were also incorporated into the evaluation. Additionally, during  $qu$  and TCS laboratory testing, axial strain readings were recorded, which were then coupled with associated stress readings to develop stress-strain curves, allowing values of  $E$  to be determined for the rock specimens.

All rock specimens were collected in the field through core-drilling techniques. Rock specimens for testing were obtained from the field samples by coring in the laboratory and exhibited a typical diameter of 2.2 inches (5.6 cm). The lithology of the rock specimens tested was consistent and consisted of



intact, fine-grained, slightly muddy limestone with very few defects such as shells and vugs. Rock specimen preparation was completed to meet shape, length-to-diameter ratio, and crystal size-to-diameter criteria in accordance with ASTM method D 4543 (ASTM, 2008a). Unconfined and triaxial compression testing of rock specimens giving  $q_u$  and TCS, respectively, were completed by ASTM method D 7012 (ASTM, 2007) or earlier versions of this standard of practice congruent to the testing time frame. A single splitting tensile test was performed under compliance with ASTM method D 3967 (ASTM, 2008b). Stress-strain curves for select rock specimens were developed, from which values of  $E$  were obtained following ASTM method D 7012 (ASTM, 2007) or earlier versions of this standard of practice.

All specimens met preparation criteria established in ASTM method D 4543 (ASTM, 2008a), with the exception of three specimens that minimally failed the length-to-diameter ratio criterion. In addition to adhering to ASTM standard practices, several criteria were also considered to ensure that acceptable testing results were obtained. Just prior to testing, the specimens were cored in the laboratory from existing FAS rock matrix samples that had been collected 4 months to 9 years earlier. As noted in several studies, rock specimens will undergo simultaneous hardening and mechanical fatigue as soon as they are removed from the ground (Kowalski, 1994). Upon its collection, a rock specimen will expand due to the relaxation of *in situ* stresses. During this expansion period, the rock specimen will harden, resulting in increased strength. The degree of this hardening phenomenon is specific to the type of rock and time lapse after its collection, as the specimen will exhibit increasing hardness with time until it reaches a maximum strength. Mechanical fatigue of a rock specimen is primarily a result of changes of atmospheric agents such as temperature, moisture, and pressure, which will impart fatigue on a rock specimen until it is disintegrated. Typically, an ongoing hardening process will impart a greater influence in increasing the strength of a rock specimen than mechanical fatigue will impart in weakening the strength of the specimen, thereby resulting in an overall net increase in strength seen during the hardening process. At completion of the hardening process, mechanical fatigue continues to slowly act and decreases the strength of the rock specimen until it is disintegrated. A discernible trend of slightly decreasing rock specimen strength is seen that is attributable to the sample collection and laboratory testing time lapse; however, any significant strength differences are likely largely due to natural strength

variations that would be expected in the FAS rock matrix.

Wet rock specimens tend to fail at lower axial loads, providing a more realistic interpretation of *in situ* rock strength for such conditions; however, this effect of decreasing strength with increasing moisture content is small, and for most engineering applications it can be disregarded (Obert and Duvall, 1967). However, Shakoor and Barefield (2009) indicated that an amplification in the reduction in strength, to a substantial level, with an increasing degree of saturation can be seen for various rock types. Also, the reduction in strength primarily occurred at moisture contents between 0 percent and 33 percent of fully saturated rock specimen conditions. Because the FAS rock core testing was completed under undrained and less than 50 percent specimen saturation conditions, excessive pore pressure likely did not accumulate during testing, as increasing pore pressure may increase the apparent strength of the rock specimen. With the specimens being wet during testing, however, any appropriate reduction in apparent strength would closely approximate *in situ* conditions. Confining pressures applied during triaxial testing of the rock specimens ranged from 60 to 400 psi (0.41 to 2.76 MPa) based on an estimated average horizontal effective stress likely seen during ASR operational conditions. The temperature of a rock specimen can also be adjusted to mimic the *in situ* temperature condition resulting from a natural geothermal gradient or other heat sources. At high temperatures, rock specimens will exhibit enhanced ductility, depressed yield strength, and a lower ultimate strength than those at lower temperatures (Handin et al., 1963; Davis, 1984). However, the *in situ* temperatures noted at the ASR sites are sufficiently low, as exhibited by the temperature of water extracted from the FAS, that temperature adjustment during rock specimen testing was not required. Based on these testing criteria, testing was performed to approximate *in situ* stress and temperature conditions encountered during ASR operational recharge and recovery phases.

A stiff testing machine coupled with a servo system was used to conduct the tests. The servo system automatically regulated the stress rate applied by the testing machine to achieve a constant strain rate of 0.03 percent/minute. This practice significantly reduced the chance for catastrophic failure of the rock specimen at or just beyond its ultimate strength, allowing stress-strain readings to be compiled substantially beyond the ultimate strength of the specimen. Additionally, the apparent strength of a rock specimen can be influenced by the rate of strain, as a rock specimen will exhibit greater strength as the

Table 1. Laboratory testing results for Floridan Aquifer System rock matrix specimens.

ASR Site	Boring Number	Depth* (ft bgs)	Time Lapse** (yr/mo)	Laboratory Test	$q_u$ (psi)	$\Phi$ (°)	$C$ (psi)
Caloosahatchee River	CCBRY	653	0/7	U/T	1,110	34.0	330
Caloosahatchee River	CCBRY	740	0/7	T	NR	36.5	760
Caloosahatchee River	CCBRY	910	0/7	U/T	415/650	34.5	450
Caloosahatchee River	CCBRY	952	0/7	U/T	1,145	34.0	360
Caloosahatchee River***	Various	932–1,324	2/0	U	NR	NR	443
Caloosahatchee River	CCBRY	733	0/4	U	486	NR	NR
Caloosahatchee River	CCBRY	851	0/4	U	1,652	NR	NR
Caloosahatchee River	CCBRY	897	0/4	U	1,145	NR	NR
Caloosahatchee River	EXBRY-1	1,305	2/0	U	1,301	NR	NR
Caloosahatchee River	EXBRY-1	1,322	2/0	U	651	NR	NR
Caloosahatchee River	EXBRY-1	1,324	2/0	U	1,843	NR	NR
Hillsboro	W-17986	1,134	9/0	U/T	330	20.0	130
Moorehaven	W-18253	875	8/0	U/T	460	30.0	210
Port Mayaca	W-18463	638	5/0	ST/U/T	1,980	32.5	440
Port Mayaca	W-18463	926	5/0	U/T	1,220	31.0	400
Kissimmee River	W-18776	656	7/0	U/T	430	13.5	175
Kissimmee River	W-18776	803	7/0	U/T	520	23.5	180
Seminole-Brighton	W-18811	693	1/6	U/T	870/1,100	36.0	265
Seminole-Brighton	W-18811	932	1/6	U/T	560	12.0	235
Paradise Run	W-18812	797	1/0	U/T	2,090	38.5	275

bgs = below ground surface;  $q_u$  = unconfined compressive strength; psi = pounds per square inch;  $\Phi$  = angle of internal friction;  $C$  = cohesion; U = unconfined compressive; T = triaxial compressive; ST = splitting tensile; NR = not recorded. 1 ft = 0.3048 m; 1 psi = 0.006895 MPa.

\*Specimens for laboratory testing typically retained within 10 ft of listed depth.

\*\*Time lapse between sample collection and laboratory testing.

\*\*\*Arithmetic mean values reported by Brown et al. (2005) for various borings to include Port Mayaca site.

rate of strain is increased. Another indicator of valid testing is the failure modes of the rock specimens. Rock specimens tested under unconfined conditions primarily exhibited longitudinal failure, along with some specimens exhibiting shear failure. Rock specimens tested under triaxial conditions primarily exhibited shear and multiple shear failure modes and to a lesser extent longitudinal failure. The rock specimen tested under the splitting tensile test failed by a single fracture splitting the specimen into two near equal-sized halves. These are typical failure modes indicating acceptable testing procedures were completed.

Testing procedures and results appear to be valid and exhibit minimal data-use uncertainty based on adherence to rock specimen preparation criteria prescribed in ASTM method D 4543 (ASTM, 2008a). Slightly lower  $q_u$  results were seen for specimens exhibiting a significant time lapse between sample collection and testing when compared to results for those exhibiting a minimal time lapse. The lower  $q_u$  values slightly reduce the arithmetic mean values for  $q_u$  and  $C$ , which will result in less calculated resistance to hydraulically induced fracturing. Rock testing and mechanical property results are summarized in Table 1. Arithmetic mean values of 998 psi (6.9 MPa), 28.9°, and 332 psi (2.3 MPa) were

determined for  $q_u$ ,  $\Phi$ , and  $C$ , respectively, to be used in the hydraulically induced fracturing evaluation methods. Arithmetic mean values for TCS and  $E$  were not determined because their magnitudes can be influenced by the confining pressure applied during testing, and substantial amounts of tests were not conducted at various confining pressures. At confining pressures ranging from 60 to 400 psi (0.41 to 2.8 MPa), the TCS of 28 specimens ranged from 350 to 11,930 psi (2.4 to 82.3 MPa). Testing results of 18 samples for the tangent modulus  $E$  ranged from  $0.33 \times 10^6$  to  $17.4 \times 10^6$  psi (2,275 to 119,969 MPa) at confining pressures ranging from 0 to 210 psi (0 to 1.5 MPa).

## DISCUSSION OF RESULTS

### Primary Methods

The predictive maximum allowable TH values and well-head pressures initiating hydraulically induced fracturing utilizing the primary methods of evaluation for each potential ASR site are shown in Table 2. Hydraulically induced fracturing, under the primary methods, can be initiated at the well borehole wall or anywhere within the FAS when the TH critical threshold level is reached at any point in the hydraulic

## Fracturing the Floridan Aquifer

Table 2. Predictive water-pressure thresholds above which hydraulic fracturing at the top of the Floridan Aquifer System may be induced.

ASR Site	Shear Method		Tensile Method				Microfracture Method			
	Well Head/FAS		Well Head				Well Head/ FAS			
	FS/No FS		FS		No FS		FS		No FS	
	TH (ft NGVD)	Pressure (psi)	TH (ft NGVD)	Pressure (psi)	TH (ft NGVD)	Pressure (psi)	TH (ft NGVD)	Pressure (psi)	TH (ft NGVD)	Pressure (psi)
Caloosahatchee River	>>400	>>164	309	125	343	139	220	86	244	97
Moorehaven	>>400	>>167	455	190	505	212	321	133	357	148
Kissimmee River	>>400	>>168	301	125	334	139	210	85	233	95
Port Mayaca	>>400	>>164	412	169	458	189	296	119	329	133
Hillsboro	>>400	>>168	503	213	559	237	356	149	395	166
Seminole-Brighton	>>400	>>163	360	146	400	163	260	102	289	115
Paradise Run	>>400	>>165	308	125	342	140	218	86	242	97

TH = total head; NGVD = National Geodetic Vertical Datum, 1929; FAS = Floridan Aquifer System; FS = factor of safety applied at 10 percent; >> = significantly greater than. 1 ft = 0.3048 m; 1 psi = 0.006895 MPa.

pressure field. However, the mechanics of hydraulically induced fracturing under the tensile method require that the TH critical threshold level be reached within the well borehole to initiate fracturing of the well borehole wall. The mechanics for the shear and microfracture methods require the TH to remain at or above the critical threshold level within the initiated fracture to impart its propagation. Hydraulically induced fracturing will not be initiated nor propagated at any TH below the critical threshold level. To reach the TH critical threshold level, injection of water into the FAS is required; however, fracture initiation and propagation can still occur during recovery if the TH remains at or above the TH critical threshold level.

The shear method evaluation results indicate that it is highly unlikely that hydraulically induced fracturing due to shear failure will occur under any probable ASR operational condition, either of the well borehole wall or within the FAS (Table 2). The tensile method evaluation results indicate that hydraulically induced fracturing due to failure of the well borehole wall is possible if ASR operations increase the TH to the predictive critical threshold levels (Table 2). Likewise, the microfracture method evaluation results indicate that hydraulically induced fracturing due to microfracture development is possible if ASR operations increase the TH to the predictive critical threshold levels (Table 2).

It should be remembered that the resultant predicted TH values shown in Table 2 are for the evaluation point of interest at the top of the FAS. The stratigraphic zone of the FAS below the evaluation point of interest requires TH values greater than those shown in Table 2 to initiate hydraulically induced fracturing, assuming the FAS rock matrix exhibits similar or greater fracture-resistant mechanical prop-

erties to those used in the evaluations. For all potential ASR sites, check method results are consistent with predictive TH values as determined using the primary methods.

Fracture gradients were developed as another alternative to illustrate and compare the  $P$  values required to initiate the onset of hydraulically induced fracturing. A fracture gradient is  $P$  in psi per foot of depth below ground surface at which the onset of hydraulically induced fracturing will be initiated. Fracture gradients were calculated by determining the  $P$  values at which the initiation of hydraulically induced fracturing is realized at the evaluation points of interest and dividing it by the thickness of strata above those points. Fracture gradients for the shear method are substantially greater than 0.73 psi/ft (0.017 MPa/m) for both no applied FS and applied FS. Fracture gradients for the tensile and microfracture methods are 0.69 and 0.61 psi/ft (0.016 and 0.014 MPa/m) for no applied FS and 0.66 and 0.59 psi/ft (0.015 and 0.013 MPa/m) for an applied FS of 10 percent, respectively. These fracture gradients were found to be consistent between all potential ASR sites. In addition, the fracture gradients estimated using the primary methods are consistent with those suggested by Ehlig-Economides and Economides (2010).

### Hydraulically Induced Fracture Propagation Arrest

The FAS contains natural discontinuities such as open fractures, fractures filled with material of negligible tensile strength, joints, bedding planes, and a horizontal contact zone with the overlying Hawthorn Group deposit. Should a hydraulically induced fracture be developed and propagate within the FAS, it is highly likely that it will align with one of

these discontinuities and be contained within the FAS. Should the fracture encounter the horizontally oriented contact zone between the FAS and Hawthorn Group deposit, it will likely propagate along the zone as the hydraulic fracture tip stress will be redistributed and align with the contact zone, following the arrest model presented by Gudmundsson and Brenner (2001). The hydraulic fracture will propagate until the hydraulic fracture tip stress is reduced to a level not conducive to overcoming fracture resisting stresses and FAS discontinuity strength.

Values of  $E$  were calculated from the rock testing program results for the FAS rock matrix; however, testing of Hawthorn Group deposit materials was not completed, and therefore values of  $E$  were not obtained. Values of  $E$  for the FAS rock matrix ranged from  $0.33 \times 10^6$  to  $17.4 \times 10^6$  psi (2,275 to 119,969 MPa). The range of values of  $E$  for the Hawthorn Group deposit materials is expected to be significantly lower than those of the FAS due to the different types of materials found in each deposit. For clay and silt materials such as those found in the Hawthorn Group deposit, typical values of  $E$  are in the range of 300 to 15,000 psi (2.1 to 103.4 MPa) (Converse, 1962; Hallam et al., 1978; Das, 1984; Hunt, 1986; Cernica, 1995; and Bowles, 1997). Modulus of elasticity values estimated for the Hawthorn Group deposit from down-hole seismic velocity data at a project site north of Lake Okeechobee (Golder Associates Incorporated, 2009) suggest values ranging from 28,000 to 42,000 psi (193.1 to 289.6 MPa) for clay- and silt-dominated samples.

Due to the Hawthorn Group deposit being significantly less stiff than the FAS, the fracture tip stress of a vertically propagating hydraulically induced fracture initiated in the FAS is likely to be effectively redistributed and dissipated in the Hawthorn Group deposit. Dissipation of the tip stress in the Hawthorn Group deposit would occur at such a level that the propagation of the hydraulic fracture would be arrested at the FAS and Hawthorn Group deposit contact, in keeping with the arrest model presented by Gudmundsson and Brenner (2001).

On the basis of the little evidence that exists about the ability of geological or anthropogenic sources to create differential stress patterns, it is considered that zones or entire stratigraphic units of the FAS and Hawthorn Group deposit are not subjected to compressive or tension stresses at quite different magnitudes. Therefore, a stress barrier or barriers that would arrest vertical propagation of a hydraulic fracture initiated in the FAS from entering the Hawthorn Group deposit is not likely.

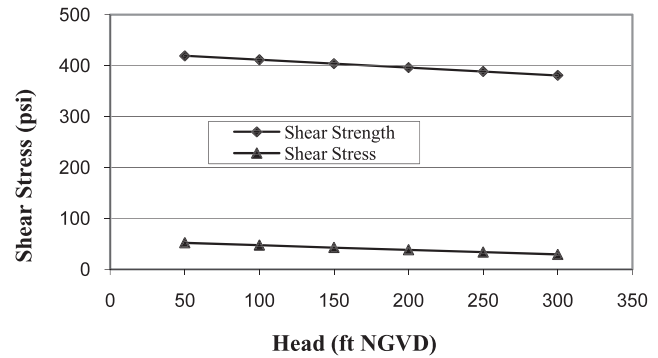


Figure 3. Predictive relation of stress in pounds per square inch (psi) and total head in feet (ft), based on the 1929 National Geodetic Vertical Datum (NGVD), for operational recharge phase using the shear method for the critical failure plane of  $59^\circ$ . 1 ft = 0.3048 m; 1 psi = 0.006895 MPa.

### APPLICATION EXAMPLE

The primary methods to evaluate hydraulically induced fracturing were applied to the potential Caloosahatchee River ASR site to illustrate development of predictive maximum allowable TH values and well-head pressure hydraulically induced fracturing thresholds. The conceptual hydrogeological model used for the evaluation of this potential ASR site consists of 32 ft (10 m) of SAS and 518 ft (158 m) of the Hawthorn Group deposit, each exhibiting an approximate specific unit weight of 130 pounds per cubic foot ( $2,082 \text{ kg/m}^3$ ) at their natural moisture content. The evaluation point of interest is the top of the FAS (i.e., 550 ft [168 m] below ground surface).

Predictive stress and head relations under recharge and recovery ASR operational phases using the shear method are shown on Figures 3 and 4, respectively. Hydraulically induced fracturing due to shear would be initiated when the magnitude of the shear stress component applied to the FAS rock matrix is equal in

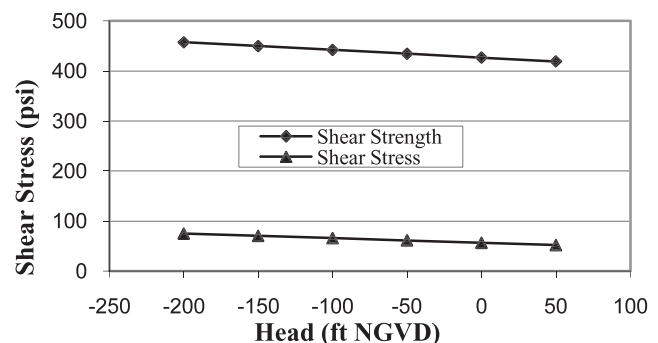


Figure 4. Predictive relation of stress in pounds per square inch (psi) and total head in feet (ft), based on the 1929 National Geodetic Vertical Datum (NGVD), for operational recovery phase using the shear method for the critical failure plane of  $59^\circ$ . 1 ft = 0.3048 m; 1 psi = 0.006895 MPa.

## Fracturing the Floridan Aquifer

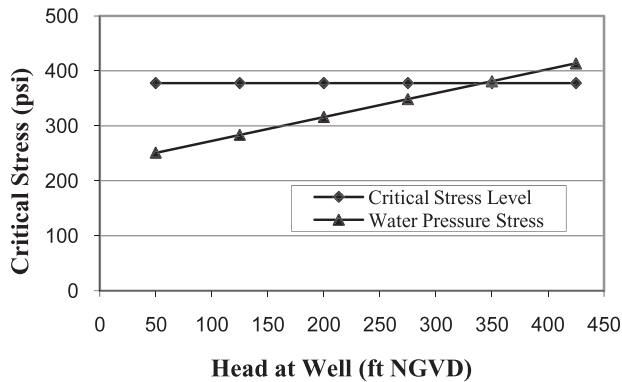


Figure 5. Predictive relation of stress in pounds per square inch (psi) and total head in feet (ft), based on the 1929 National Geodetic Vertical Datum (NGVD), for operational recharge phase using the tensile method. 1 ft = 0.3048 m; 1 psi = 0.006895 MPa.

magnitude to the shear strength component of the FAS rock matrix (i.e., on Figures 3 and 4, the shear stress line would intercept the shear strength line). As illustrated on Figures 3 and 4, respectively, the shear trend lines will converge at very high TH values under the recharge phase, while they diverge under the recovery phase. These trends show that it is extremely unlikely that ASR operational recharge and recovery conditions will be met to initiate the onset of hydraulically induced fracturing within the well bore and/or FAS. If hydraulically induced fracturing due to shear were to occur, the critical shear failure plane would likely align at a  $\theta$  angle of  $59.5^\circ$  measured from the horizontal.

The predictive stress and head relations under the ASR operational recharge phase using the tensile method are shown on Figure 5. Hydraulically induced fracturing of the well borehole wall would initiate when the magnitude of the  $P$  stress component in the well borehole equals the magnitude of the critical stress level (i.e., on Figure 5, the intercept of the water-pressure stress line and the critical stress level). It can be determined from Figure 5 that hydraulic fracturing may be initiated and propagated when the TH value within the well borehole reaches or exceeds approximately 343 ft (105 m) National Geodetic Vertical Datum (NGVD). However, hydraulic fracturing is not a concern at levels under this TH.

Predictive HDR and head relations under the recharge phase derived from the microfracture method are shown on Figure 6. Hydraulically induced microfracturing of the FAS rock matrix would be initiated and maintained when the ratio of the  $P$  stress component to the total horizontal stress component, the HDR, is equal to and greater than the LHDR, set at 0.8 (i.e., on Figure 6, the HDR line

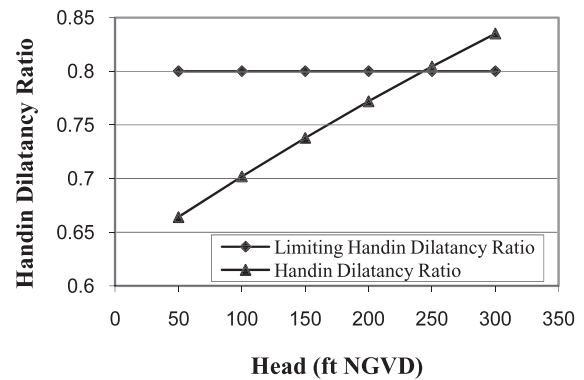


Figure 6. Predictive relation of the Handin Dilatancy Ratio (HDR) and total head in feet (ft), based on the 1929 National Geodetic Vertical Datum (NGVD), for operational recharge phase using the microfracture method. 1 ft = 0.3048 m; 1 psi = 0.006895 MPa.

would intercept and project above the LHDR line). It can be determined from this figure that hydraulically induced microfracturing will potentially be initiated and maintained under the ASR operational recharge phase when the TH within the well bore and/or FAS reaches and exceeds approximately 244 ft (74 m) NGVD. However, microfracture initiation is not a concern at levels under this TH.

## CONCLUSIONS

Three primary methods, termed shear, tensile, and microfracture, based on relationships of FAS rock matrix mechanical properties and *in situ* stresses were applied to determine the  $P$  values that would induce hydraulic fracturing at the top of the FAS. Shear method results indicate that an extremely high  $P$  in the FAS is required to initiate fracturing by shear failure. Tensile method results indicate that a relatively moderate  $P$  is required to initiate fracturing by tensile splitting of the well borehole wall. Microfracture method results indicate that a moderately low  $P$  is required to initiate fracturing. It is unlikely that extremely high  $P$  values will be achieved during ASR operation; therefore, hydraulic fracturing due to shear failure is not a concern. However, moderate  $P$  values can potentially be achieved, initiating hydraulic fracturing due to tensile splitting of the well borehole wall. More likely, moderately low  $P$  values causing microfracture initiation may be achieved within practical ASR operational limits (Table 2). Two additional hydraulically induced fracturing methods were applied and produced results consistent with the three primary methods, providing for increased assurance of the predictive  $P$  values that may induce fracturing.

Hydraulically induced fracturing can be initiated at and propagate from the well borehole wall for all three fracture mechanisms, while the ability to initiate and propagate hydraulic fracturing away from the borehole wall and within the FAS can be achieved by shear failure and microfracture development. Hydraulically induced fracturing is not a concern at any  $P$  below the critical threshold level that may result from practical ASR operation. If the critical water-pressure threshold is met for the top of the FAS, fracturing is more likely to occur there rather than in deeper portions of the FAS, as increasing overburden stress with depth will largely negate fracture-inducing stresses. If hydraulically induced fracturing of the FAS rock matrix is initiated, it will likely be vertically oriented; however, orientation and propagation may be influenced by anisotropy, planar inhomogeneities, or alignment of the principal stresses in the FAS.

Potential for hydraulically induced fracturing of the Hawthorn Group deposit, due to vertically upward propagating fractures initiated in the FAS, is very unlikely. These type of fractures initiated in the FAS would be arrested at or re-directed along the discontinuity formed by the interface of the FAS and Hawthorn Group deposit. If the fracture were able to propagate through the discontinuity and into the Hawthorn Group deposit, the softer nature of the Hawthorn Group deposit would arrest its propagation. It is likely that significant stress barriers are not present in the FAS and Hawthorn Group deposit, therefore stress barriers do not provide an arrest mechanism for hydraulically induced fracture propagation.

#### ACKNOWLEDGMENTS

We thank June Mirecki and Orlando Ramos-Gines of the U.S. Army Corps of Engineers, Jacksonville District, and Robert Verrastro and Emily Richardson of the South Florida Water Management District, for their support and reviews, which greatly enhanced this manuscript. Also, we would like to thank the three anonymous *Environmental & Engineering Geoscience* reviewers for their valuable comments that significantly improved this manuscript.

#### REFERENCES

- AADNOY, B. S., 1996, *Modern Well Design*: A. A. Balkema, Rotterdam, Netherlands, 250 p.
- ALEHOSSEIN, H. AND BOLAND, J. N., 2004, Strength, toughness, damage and fatigue of rock. In Atrens, A.; Boland, J. N.; Clegg, R.; and Griffiths, J. R. (Editors), *Structural Integrity and Fracture*: Australia Fracture Group Inc., Brisbane, Australia, pp. 1–8.
- AMERICAN SOCIETY FOR TESTING AND MATERIALS (ASTM), 2007, *Standard Test Method for Compressive Strength and Elastic Moduli of Intact Rock Core Specimens under Varying States of Stress and Temperature, D 7012-07*: American Society for Testing and Materials, West Conshohocken, PA, 8 p.
- ASTM, 2008a, *Standard Practices for Preparing Rock Core as Cylindrical Test Specimens and Verifying Conformance to Dimensional and Shape Tolerances, D 4543-08*: American Society for Testing and Materials, West Conshohocken, PA, 9 p.
- ASTM, 2008b, *Standard Test Method for Splitting Tensile Strength of Intact Rock Core Specimens, D 3967-08*: American Society for Testing and Materials, West Conshohocken, PA, 4 p.
- BLYTH, F. G. H. AND DE FREITAS, M. H., 1984, *A Geology for Engineers*, 7th ed.: Elsevier, Amsterdam, Netherlands, 336 p.
- BOUWER, H., 1978, *Groundwater Hydrology*: McGraw-Hill, New York, NY, 480 p.
- BOWLES, J. E., 1997, *Foundation Analysis and Design*, 5th ed.: McGraw-Hill, New York, NY, 1207 p.
- BROWN, C. J., 2007, A stochastic evaluation of the subsidence potential of the Hawthorn Group in south Florida as a result of the CERP ASR system. In Fox, P. (Editor), *Proceedings of the 6th International Symposium on Managed Artificial Recharge of Groundwater, ISMAR6*: Acacia Publishing Inc., Phoenix, AZ, pp. 590–600.
- BROWN, C. J.; ITANI, S.; AND ZHANG, M., 2005, *Final Draft Aquifer Storage & Recovery Regional Study: A Scientific Evaluation of Potential Pressure Induced Constraints and Changes in the Floridan Aquifer System and the Hawthorn Group*: U.S. Army Corps of Engineers Report, Jacksonville, 71 p.
- CERNICA, J. N., 1995, *Geotechnical Engineering: Soil Mechanics*: John Wiley & Sons, New York, NY, 480 p.
- CONVERSE, F. J., 1962, *Foundation Engineering*: McGraw-Hill, New York, NY, 1146 p.
- DAS, B. M., 1984, *Principles of Foundation Engineering*: PWS-Kent Publishing Company, Boston, MA, 595 p.
- DAVIS, G. H., 1984, *Structural Geology of Rocks and Regions*: John Wiley & Sons, New York, NY, 492 p.
- DOMENICO, P. AND SCHWARTZ, F., 1998, *Physical and Chemical Hydrogeology*, 2nd ed.: John Wiley & Sons, New York, NY, 506 p.
- DRISCOLL, F. G., 1986, *Groundwater and Wells*, 2nd ed.: Johnson Filtration Systems Inc., St. Paul, MN, 1089 p.
- EHLIG-ECONOMIDES, C. AND ECONOMIDES, M., 2010, Sequestering carbon dioxide in a closed underground volume: *Journal of Petroleum Science and Engineering*, Vol. 70, No. 1–2, pp. 123–130.
- FERNALD, E. A. AND PURDUM, E. D., 1998, *Water Resources Atlas of Florida*: Institute of Science and Public Affairs, Florida State University, Tallahassee, FL, 310 p.
- FJAR, E.; HOLT, R. M.; HORSRUD, P.; RAAEN, A. M.; AND RISNES, R., 2008, *Petroleum Related Rock Mechanics*, 2nd ed.: Elsevier, Amsterdam, Netherlands, 514 p.
- GOLDER ASSOCIATES INCORPORATED, 2009, *Downhole Geophysical Investigation Data, Okeechobee Landfill*: Golder Associates Incorporated, unpublished, Jacksonville, 125 p.
- GOODMAN, R. E., 1980, *Introduction to Rock Mechanics*: John Wiley & Sons, New York, NY, 478 p.
- GUDMUNDSSON, A. AND BRENNER, S. L., 2001, How hydrofractures become arrested: *Terra Nova*, Vol. 13, No. 6, pp. 456–462.
- HAIMSON, B. C., 1978, Effect of cyclic loading on rock. In Silver, M. L. and Tiedemann, D. A. (Editors), *Dynamic Geotechnical Testing, ASTM STP 654*: American Society for Testing and Materials, West Conshohocken, PA, pp. 228–245.
- HALLAM, M. G.; HEAF, N. J.; AND WOOTTON, L. R., 1978, *Dynamics of Marine Structures, Report UR 8*, 2nd ed.: CIRIA Underwater Engineering Group, London, U.K., 326 p.

- HANDIN, J.; HAGER, R. V.; FRIEDMAN, M.; AND FEATHER, J. N., 1963, Experimental deformation of sedimentary rocks under confining pressure: Pore pressure tests: *Bulletin American Association of Petroleum Geologists*, Vol. 47, No. 11, pp. 717–755.
- HEIDBACH, O.; TINGAY, M.; BARTH, A.; REINECKER, J.; KURFEB, D.; AND MÜLLER, B., 2008, *The 2008 Release of the World Stress Map*: Electronic document, available at [www.world-stress-map.org](http://www.world-stress-map.org)
- HIGDON, A.; OHLSEN, E. H.; STILES, W. B.; WEESE, J. A.; AND RILEY, W. F., 1985, *Mechanics of Materials*, 4th ed.: John Wiley & Sons, New York, NY, 744 p.
- HUBBERT, M. K. AND WILLIS, D. G., 1957, Mechanics of hydraulic fracturing: *Transactions Society of Petroleum Engineers, AIME*, Vol. 210, pp. 153–166.
- HUNT, R. E., 1986, *Geotechnical Techniques and Practices*: McGraw-Hill, New York, NY, 729 p.
- JAEGER, J. C.; COOK, N. G. W.; AND ZIMMERMAN, R. W., 2007, *Fundamentals of Rock Mechanics*, 4th ed.: Blackwell Publishing Ltd., Malden, MA, 475 p.
- KEITH, L. A. AND RIMSTDT, J. D., 1985, A numerical compaction model of overpressuring in shales: *Mathematical Geology*, Vol. 17, No. 2, pp. 115–135.
- KOWALSKI, W. C., 1994, Controversy: Mechanical fatigue or hardening of rocks after their excavations: *Bulletin International Association of Engineering Geology*, Vol. 50, pp. 51–57.
- MILLER, J. A., 1986, *Hydrogeologic Framework of the Floridan Aquifer System in Florida and in Parts of Georgia, Alabama, and South Carolina*: U.S. Geological Survey Water-Resources Investigation Report 1403-B, 91 p.
- OBERT, L. AND DUVALL, W. I., 1967, *Rock Mechanics and the Design of Structures in Rock*: John Wiley & Sons, New York, NY, 650 p.
- PALCIAUSKAS, V. V. AND DOMENICO, P., 1980, Microfracture development in compacting sediments: Relation to hydrocarbon-maturation kinetics: *Bulletin American Association of Petroleum Geologists*, Vol. 64, No. 6, pp. 927–937.
- POLLARD, D. D. AND AYDIN, A., 1988, Progress in understanding jointing over the past century: *Geological Society America Bulletin*, Vol. 100, pp. 1181–1204.
- POLLARD, D. D.; SEGAL, P.; AND DELANY, P. T., 1982, Formation and interpretation of dilatants echelon cracks: *Geological Society America Bulletin*, Vol. 93, pp. 1291–1303.
- RAHN, P. H., 1986, *Engineering Geology: An Environmental Approach*: Elsevier, New York, NY, 589 p.
- REESE, R. S., 2000, *Hydrogeology and the Distribution of Salinity in the Floridan Aquifer System, Southwestern Florida*: U.S. Geological Survey Water-Resources Investigation Report 98-4253, 86 p.
- RUTQVIST, J. AND STEPHANSSON, O., 2003, The role of hydromechanical coupling in fractures rock engineering: *Hydrogeology Journal International Association Hydrogeologists*, Vol. 11, No. 1, pp. 7–40.
- SCOTT, T. M., 2001, *Text to Accompany the Geologic Map of Florida*: Florida Geological Survey Open-File Report 80, 28 p.
- SHAKOOR, A. AND BAREFIELD, E. H., 2009, Relationship between unconfined compressive strength and degree of saturation for selected sandstones: *Environmental Engineering Geoscience*, Vol. XV, No. 1, pp. 29–40.
- SHERMAN, W. C., 1973, Elements of soil and rock mechanics. In Cummins, A. B. and Given, I. A. (Editors), *SME Mining Engineering Handbook, Vol. 1, Chapter 6*: Society of Mining Engineers, New York, NY, pp. 1–52.
- SINGH, S. K., 1989, Fatigue and strain hardening behavior of graywacke from the Flagstaff Formation, New South Wales: *Engineering Geology*, Vol. 26, pp. 171–179.
- SMITH, S. A., 1989, *Manual of Hydraulic Fracturing for Well Stimulation and Geologic Studies*: National Water Well Association, Dublin, OH, 66 p.
- STERRETT, R. J., 2007, *Groundwater and Wells*, 3rd ed.: Johnson Screens, A Weatherford Company, New Brighton, MN, 812 p.
- TERZAGHI, K. AND PECK, R. B., 1967, *Soil Mechanics in Engineering Practice*, 2nd ed.: John Wiley & Sons, New York, NY, 729 p.
- U.S. ARMY CORPS OF ENGINEERS (USACE) AND SOUTH FLORIDA WATER MANAGEMENT DISTRICT (SFWMD), 1999, *Central and Southern Florida Project Comprehensive Review Study, Final Feasibility Report and Programmatic Environmental Impact Statement*: U.S. Army Corps of Engineers and South Florida Water Management District Report, Jacksonville, 590 p.
- ZHANG, P.; XU, J.; AND LI, N., 2008, Fatigue properties analysis of cracked rock based on fracture evolution process: *Journal Central South University Technology*, Vol. 15, pp. 95–99.